Application of thematic mapper images to determine regional evaporation from the playas in the Western Desert of Egypt

W.G.M. Bastiaanssen
M.H. Abd El Karim

Report 31

The WINAND STARING CENTRE, Wageningen (The Netherlands), 1990

ABSTRACT

Bastiaanssen, W.G.M. & M.H. Abd El Karim, 1990. Application of thematic mapper images to determine regional evaporation from the playas in the Western Desert of Egypt.
Wageningen, The Netherlands, Staring Centre. Report 31.
29 pages; 8 figs.; 4 tables.

Groundwater basins are formed in sandstone horizons, which occupy 2 million km^2 in Northeast Africa. These extensive aquifer systems contain large resources of groundwater suitable for agricultural and domestic use. Evaporation of this groundwater takes place in the depressions with a shallow groundwater table i.e. playa (En.) or sebkha (Ar.). This has consequences for the availability of groundwater.

To estimate actual evaporation from playas or sebkhas, recently a technique based on analysis of LANDSAT Thematic Mapper images and field measurements has been developed. Surface reflectance and surface temperature are obtained with Thematic Mapper measurements. Effective properties of non-homogeneous land surfaces, could be derived from the satellite image. This information can be applied to classify soils and to determine the transfer of sensible and latent heat into the atmosphere.

An algorithm has been developed to obtain maps of latent heat flux with measurements of surface reflectance and surface temperature on a pixel by pixel basis. The so obtained values are validated with ground based observations of latent heat flux, obtained by means of the Bowen-ratio energy balance method. Combination of daily evaporation values, calculated by means of models to simulate soil water flow through the unsaturated zone, with instantaneous latent heat flux values, gives maps of daily and annual evaporation rates. The overall conclusion was that evaporation from playas is significantly higher than previously estimated. This has an important impact on the total regional groundwater balance, the hydrogeological schematization and the potential of groundwater development schemes.

Keywords: groundwater, energy balance, remote sensing.

ISSN 0924-3062

This report was submitted to the symposium "Application of Remote Sensing in Hydrology and Water Resources", 12-18 March, 1990, Damascus, Syria.

The WINAND STARING CENTRE for Integrated Land, Soil and Water Research,
Postbus 125, 6700 AC Wageningen (The Netherlands).
Phone: +31837019100; fax: +31837024812; telex: 75230 VISI-NL

The WINAND STARING CENTRE is continuing the research of:
Institute for Land and Water Management Research (ICW), Institute for Pesticide Research, Environment Division (IOB), Dorschkamp Research Institute for Forestry and Landscape Planning, Division of Landscape Planning (LB), and Soil Survey Institute (STIBOKA).

INHOUD

1 INTRODUCTION

More than 96% of the Egyptian territory is desert. The magnitude of the problem of desertification is one of the major challenges facing the Government. In past years efforts have been directed to spread out the Nile Valley to reclaim desert lands. The 1977 United Nations conference on desertification recommended a feasibility study of the Nubian Sandstone aquifer system in North East Africa (2 million km^2). The objectives of this project titled "Major Regional Aquifer in NE-Africa", covering parts of Egypt, Sudan, Lybia and Chad, was to determine the hydrological characteristics of the Nubian Sandstone aquifer and the best groundwater utilization for control of desertification through land and water development. Water development plans require a proper knowledge of the different terms of the groundwater balance, particularly evaporation. Evaporation takes place in natural depressions with a shallow groundwater table (Menenti, 1984). In order to estimate the regional evaporation from the sebkhas of the Western Desert of Egypt, a research project was started in 1986.

Images from Earth Observation Satellites are available since 1972 (LANDSAT). Many studies have demonstrated the application of LANDSAT imagery for conducting inventories and for mapping various natural resources. The latter is directly related to a scarcity of available resources data like the hydrological conditions in the natural depressions. The LANDSAT Thematic Mapper measure the reflected shortwave solar radiation and emitted longwave radiation (temperature). Surface reflectance and surface temperature could be applied to classify soil types and related regional evaporation (Bastiaanssen and Menenti, 1989).

Field experiments to study the process of evaporation in highly structured hot saline soils have been carried out at different sites in the Qattara depression during five field campaigns (1986-1989). Data have been collected to study soil/atmospherical properties and surface energy fluxes. Soil samples have been collected to obtain the soil hydraulic properties. In this paper, an example of the calculation of evaporation losses in the Western Desert of Egypt by means of an integrated approach using remote sensing techniques, hydrological models and field measurements is presented.

2 GROUNDWATER RESOURCES IN THE WESTERN DESERT OF EGYPT

2.1 Groundwater systems

The Western Desert has a wide extension, most of the geological periods from Precambrian to recent are represented in the area. The regional tip of all aquifers is to the North. Older units crop out in the South while younger deposits appear gradually to the North. According to the distribution of the major uplifts, the Western Desert could be divided into four main basins (Fig. 1):

- Dakhla basin
- Plateau basin
- Ain Dalla basin
- Northwestern basin

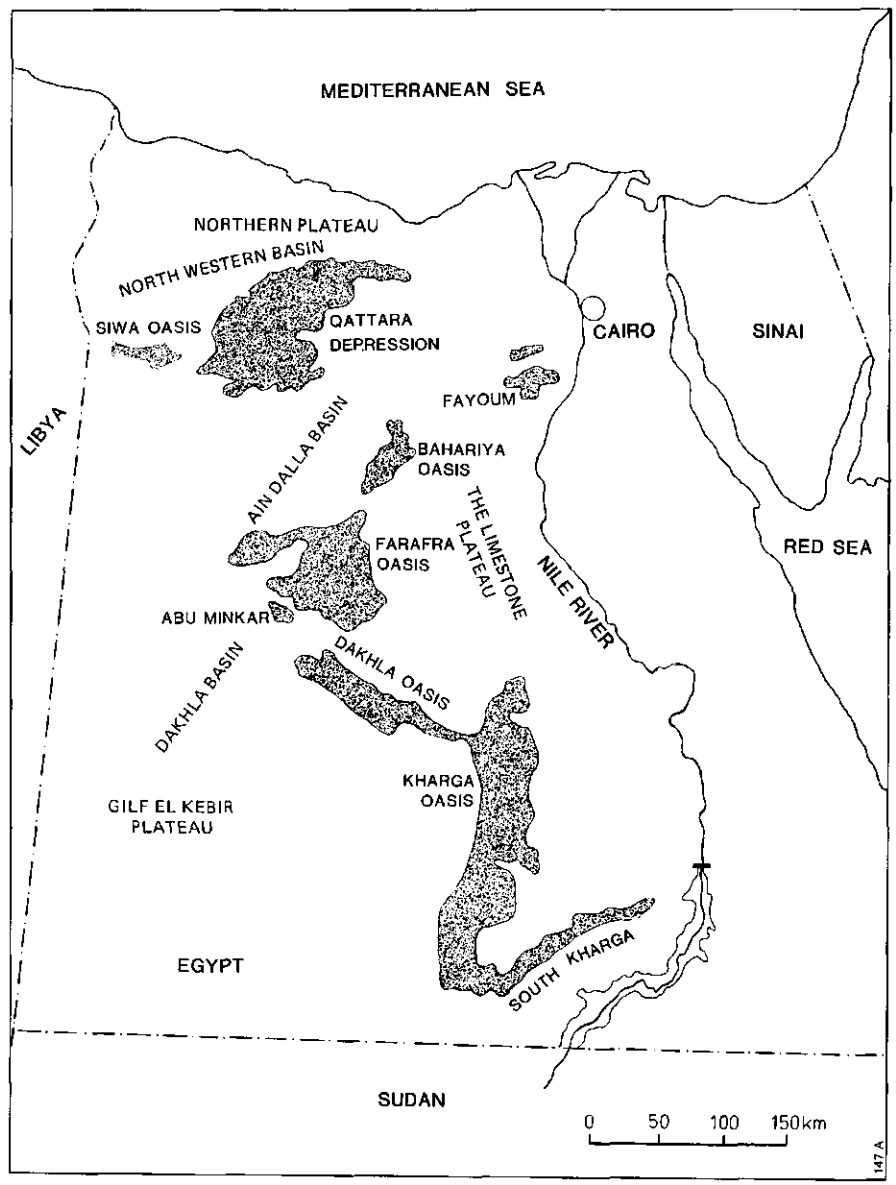

Fig. 1. Location of the main basins of the Western Desert of Egypt.

The Nubian Sandstone aquifer system consists mainly of Nubian sandstone which is coarse to medium grained, cross-bedded and contains conglomeratic beds near the base. The thickness varies from a few hundred meters in the South to 4000 meters West of Abu Mongar. This aquifer system is intercalated by shales, silt and claybeds. The Nubian Sandstone aquifer system is considered unconfined in the southern part of Egypt, while it becomes generally confined Northwards with artesian wells in the major depressions and oases. The depth of the water table varies from a few centimeters to 100 meter or more. The trend of groundwater flow in generally to North and North-East.

It is difficult to obtain more than a sketchy idea of aquifer characteristics of the Nubian Sandstone aquifer system. This is because the data tend to occur in clusters at oases and close to the Nile valley. Most of the wells are partially penetrating and hydraulic conductivity has been obtained by dividing the transmissivity by screen length only. The average hydraulic conductivity in the Western Desert varies between 1 and 10 $m.d^{-1}$ (JVO, 1981). A better understanding of recharge and discharge patterns is required to assess groundwater resources.

2.2 Recharge of groundwater

Carbon-14 dating of the groundwater of Dakhla and Kharga oases indicated that groundwater was recharged 8000-20,000 years ago. This large spread in estimated ages is due to mixing of water infiltrated during the last pluvial (6000-8000 years B.C.) with older water accumulated during the deposition of the Nubia Sandtone aquifer system (Lower Cretaceous-Jurassic age more than 67 million years ago) and recent water. Modern recharge to the aquifer probably occurs in Wadi Howar (Sudan), the humid Tibesti-Ennedi mountains (Chad) and from present rainfall in Jebel Uweinat (1-3 $mm.yr^{-1}$). Since water is infiltrated in previous times during rising of the sea level, parts of the aquifer system consists of saline water. Some parts of the natural depressions are connected to the alluvians of the Nile through the Miocene Moghra aquifer (Sundborg and Nilsson, 1985).

2.3 Natural and artificial discharge of groundwater

Natural discharge occurs from the aquifers through springs, sebkhas, oases and submarine discharge. There are fine inhabitated oases like Kharga, Dakhla, Bahariya, Farafra and Siwa in the Western Desert of Egypt. These oases are established since thousands of years. Life and agriculture have been supported by flowing wells, springs and hand dug wells. Table 1 gives a brief description of the natural and artificial losses from the oases.

The artificial discharge in the Nubian aquifer occurs from approximately 1700 shallow wells and 460 deep production wells in oases (Heinl and Brinkmann, 1989). Natural groundwater losses were previously estimated on the basis of model calibration. This implies that the estimation of

Table 1 Groundwater losses of the main depressions in the Western Desert of Egypt (after RIGW-WSC, 1989, and Brinkmann et al., 1987).

Location	Natural losses ($Mm^3.yr^{-1}$)	Artificial extraction ($Mm^3.yr^{-1}$)	
	1988	1980	1988
Bahariya oasis	23.8	33.9	40.0
Farafra oasis and Abu Mongar	15.4	1.9	152.6
Dahkla oasis	32.0	222.4	280.5
Kharga oasis	34.0	93.3	126.7
Siwa oasis	28.3	65.9	103.1
South Qattara depression (25% of total depression)	90.0	-	-
	223.5	417.4	702.9

natural losses as presented in Table 1 are by no means measured quantities and that the value 223.5 $Mm^3.yr^{-1}$ is not accurate. Consideration of the evaporation from the entire Qattara depression will considerably increase the total amount of natural losses. Reclamation projects would change the groundwater flow pattern over a period of time and decrease the natural losses by drawdown of the water table. An in-depth study on the processes and quantification of evaporation from sebkhas has been carried out. Especially the relation between evaporation and the depth of the (variable) water table has been investigated. The Qattara depression has been selected as a suitable study area.

3 FEATURES OF SEBKHAS

3.1 Occurrence of sebkhas

The Qattara depression (20.000 km^2) is situated in the northwestern part of the Western Desert of Egypt (see Fig. 1). It starts 90 km South of El Alamein and continues to the Southwest. The depression is bounded to the North and West by an escarpment up to 250 meter height. Springs with extreme saline water along the foot of the escarpment may be related to faults in the aquifer system. The southern part of the depression is open. The depression floor is covered by gravel and sand capping the Miocene Moghra aquifer. Its mean elevation is 60 meter below mean sea level (MSL). The lowest point is -134 meter -MSL (Ball, 1931). The area below sea level is 18,500 km^2. The depression is dominated by three types of deposits: alluvial fans, gravels and sebkhas. About 30% of the depression is covered by sebkhas. Sebkha is a mixture of sand and salt cristals with varying soil water content and surface roughness.

Table 2 Nomenclature of different types of sebkha.

Name	Description	Remarks
Brine	salt saturated water	pool
Salt floes, bright salt crust, white salt crust	pure white salts	semi-open pool closed pool
Dry salt crust	older pure salt crust	evaporated pool
Soft salt marsh	wet mixture sand/salts spores of cristals	fringe open water
Soft/wet sebkha, wet puffy, salty flats, fluffy, buffy	wet mixture sand/salts	extreme shallow groundwater
Dry sebkha, dry puffy, hard salt crust	dry mixture sand/salts	shallow groundwater
Rough sebkha, hummocky, very rough salt crust	dry mixture sand/salts rough polygons, cristals	transition between pool-sand

Subdivision of sebkhas gives a usefull basis for understanding the hydrological situation. The type of sebkha is related to the depth of the shallow water table since salinization is due to the rate of evaporation or soil capillary flow. Several types of sebkha could be distinguished (Table 2).

A strong variation of salinity can be observed in the vertical direction of a sebkha soil profile (Fig. 2). The highest salt concentration occurs in the dry topsoil where water is in the vapour phase. Below the liquid-vapour interface or so called evaporation front (Menenti, 1984), water is in the liquid phase and the soil is wet (Fig. 2). There is a rapid transition with depth from dry to wet. Salts are transported by the steady state soil water flow from shallow (saline) groundwater upwards and accumulate at the evaporation front. The average electric conductivity of the ground-

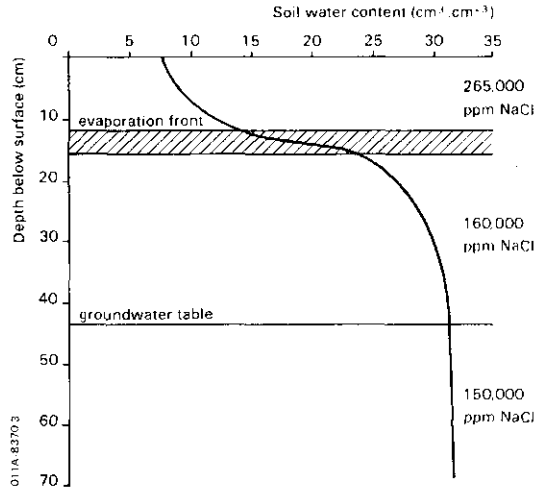

Fig. 2 Vertical distribution of soil water content and solute concentration in a puffy-type sebkha soil.

water varies between 50 and 250 mS.cm^{-1} which corresponds respectively with 28,000 and 150,000 ppm NaCl. The density of soil water in sebkhas is significantly higher than of fresh water; from 1066 kg.m^{-3} for puffy soils to 1114 kg.m^{-3} for hummocky soils and 1193 kg.m^{-3} for water in brine pools (field measurements at Bir Qifar, September 1989). This means that brines are saturated with NaCl solutes.

3.2 Classification of sebkhas with Thematic Mapper data

Classes of sebkha deposits are defined in a meaningful way on the basis of their physical and mineralogical properties. The natural variation of their spectral reflectance characteristics can be applied to identify sebkha types by remote sensing techniques. LANDSAT Thematic Mapper data are markedly superior to LANDSAT Multi Spectral Scanner because spatial resolution and surface temperature data are an essential information on the energy balance of the land surface. In order to produce a soil map, the classification results have to be supported by data from field surveys and laboratory analyses. LANDSAT Thematic Mapper scenes give a good description of the different types of sebkha. Thematic Mapper spectral bands 3, 4 and 7 gives a clear distinction between Moghra formation and sebkha deposits (List et al., 1989). Thematic Mapper band 5 provides additional information for separation in the wetter areas (Timmerman, 1989). Roeters (1987) concluded that LANDSAT Thematic Mapper bands 3, 4 and 7 are also suitable to detect different types of salt crust and related soil water content. Recently, classifications on the basis of surface temperature in combination with reflectance has given positive results (Menenti et al., 1986; Zeeman, 1989). The thermal behaviour of the surface depends mainly on the surface reflectance as outlined by Menenti et al. (1989). Different types of sebkha as presented in Table 2 can be mapped therefore using LANDSAT Thematic Mapper images in combination with ground control measurements.

4 DETERMINATION OF THE LATENT HEAT FLUX FROM THE SURFACE ENERGY BALANCE

The energy budget at the soil surface is formally written as:

$$Q^* + H + \lambda E + G_0 = 0 \qquad (W.m^{-2}) \tag{1}$$

where Q^* ($W.m^{-2}$) is the net radiation, H ($W.m^{-2}$) the sensible heat flux, λE ($W.m^{-2}$) the latent heat flux and G_0 ($W.m^{-2}$) the soil heat flux at the soil surface. When water evaporates at the evaporation front inside the soil, the soil heat flux at the evaporation front (G_e) differs from G_0. Fluxes towards the surface are counted positive. The net amount of radiant energy received by the earth's surface per unit time and area is called net radiation and can be written as:

$$Q^* = (1 - \alpha_0)K\downarrow + \epsilon'\sigma T_a^4 - \epsilon\sigma T_0^4 \qquad (W.m^{-2}) \tag{2}$$

where α_0 (-) is the surface reflectance, $K\downarrow$ ($W.m^{-2}$) the shortwave solar radiation, $\epsilon'\sigma T_a^4$ ($W.m^{-2}$) the longwave sky emittance and $\epsilon\sigma T_0^4$ the longwave surface emittance. The turbulent sensible heat flux can be written as:

$$H = - \frac{\rho_a \, C_p}{r_{ah}} (T_0 - T_a) \qquad (W.m^{-2}) \tag{3}$$

where ρ_a ($kg.m^{-3}$) is the moist air density, C_p ($J.kg^{-1}.K^{-1}$) the air specific heat and r_{ah} ($s.m^{-1}$) the mean turbulent heat transfer resistance. Substituting Eqn. (2) and Eqn. (3) into Eqn. (1) gives:

$$\lambda E = (1-\alpha_0)K\downarrow + \epsilon'\sigma T_a^4 - \epsilon\sigma T_0^4 + \frac{\rho_a \, C_p}{r_{ah}} T_a - \frac{\rho_a \, C_p}{r_{ah}} T_0 - G_e \qquad (W.m^{-2}) \tag{4}$$

Out of the variables mentioned, only α_0 and T_0 can be remotely measured. The remaining values have to be measured at standard stations and obtained from the relationship between α_0 and T_0 (Menenti et al., 1989).

5 APPLICATIONS OF LANDSAT THEMATIC MAPPER TO DETERMINE THE REGIONAL EVAPORATION FROM THE SEBKHAS IN THE WESTERN DESERT OF EGYPT

5.1 Instantaneous values

From Eqn. (4), evaporation at non-homogeneous land types (i = 1, 2, .. n) can be expressed as a function of both constant ($K\downarrow$, T_a, G_e) and variable ($\alpha_0(i)$, $T_0(i)$) meteorological parameters. The aerodynamic resistance in this case (r_{ah}) is obtained by applying the procedure of Menenti and Bastiaanssen (1989), considering the effective turbulent heat transfer as mean effective value for a specific area, in our case a quarterscene of a LANDSAT Thematic Mapper image. For the area covered by the Thematic Mapper image of 13 November 1987 (frame 179/39-40), a mean r_{ah}-value of r_{ah} = 119 $s.m^{-1}$ was obtained. Values of $K\downarrow$, T_a and G_e were measured simultaneously with the moment of satellite overpass, in the field. The spatial variation of G_e at this recording time is small so that it can be assumed to be constant for the entire area covered by the image. Substituting $K\downarrow$ = 475 $W.m^{-2}$, T_a = 18.2°C, G_e = 35 $W.m^{-2}$ and r_{ah} = 119 $s.m^{-1}$ into Eqn. (4), gives the algorithm looked for:

$$\lambda E(i) = 3657 - \alpha_0(i) * 475 - 5.5 * 10^{-8} T_0(i)^4 - 10.1 T_0(i) \quad (W.m^{-2}) \quad (5)$$

To obtain the surface reflectance from satellite data, a correction to planetary reflectance is applied for atmospheric effects (Menenti, 1984; Abd El Karim, 1989; Michels, 1989). Surface reflectance could be calculated from field measurements using solarimeters and planetary spectral reflectance measured by the Thematic Mapper sensor. The resulting satellite image of surface reflectance of an area in the Qattara depression (Bir Qifar) is shown in Figure 3.

The open water area can be detected as the area with pixels having a surface reflectance α_0 = 0.05. At-satellite temperatures as measured in band 6 of Thematic Mapper, has to be corrected into at-surface temperature values according field measurements and atmospherical correction procedures (Price, 1982; Menenti, 1984). Doing so, the following image, covering the same area as Figure 3, was obtained (Figure 4).

The latent heat image depicted in Figure 5 could be calculated with the α_0 and T_0-values (Figs. 3 and 4) by applying Eqn. (5).

Dry and wet areas can be easily discriminated. Such locations, especially when they are close to each other, are suitable to verify the λE-algorithm (Eqn. (5)). It appears that the sand dunes have nearly no evaporation while the lake shows potential evaporation values (241-361 $W.m^{-2}$). The transition from dry to wet is gradually and corresponds with transition from low to high λE-values. This proves that the algorithm developed can be applied for non-homogeneous surface types for the place and moment under consideration. A wider area of the same latent heat image is presented in Figure 6.

The sebkha deposits e.g. Qaneitra Muhasas, Bir Hussein, Qara oasis and Bir Qifar are conspicuous. Although the time scale of the latent heat flux values differ from the time scale of the natural losses as presented in

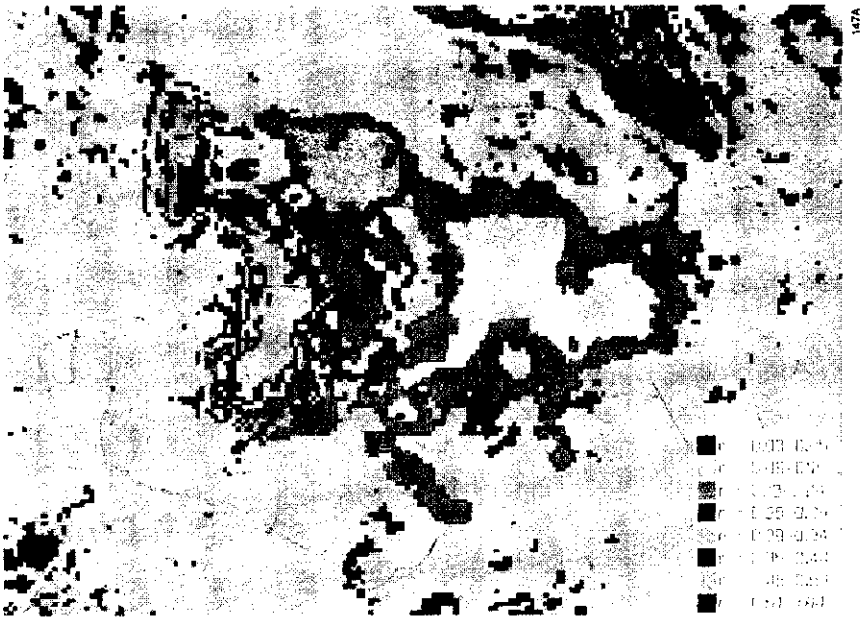

Fig. 3. Map of total surface reflectance, r, (albedo) obtained from LANDSAT Thematic Mapper observations of the Qattara depression, Western Desert of Egypt (13-11-1987, frame 179/39-40).

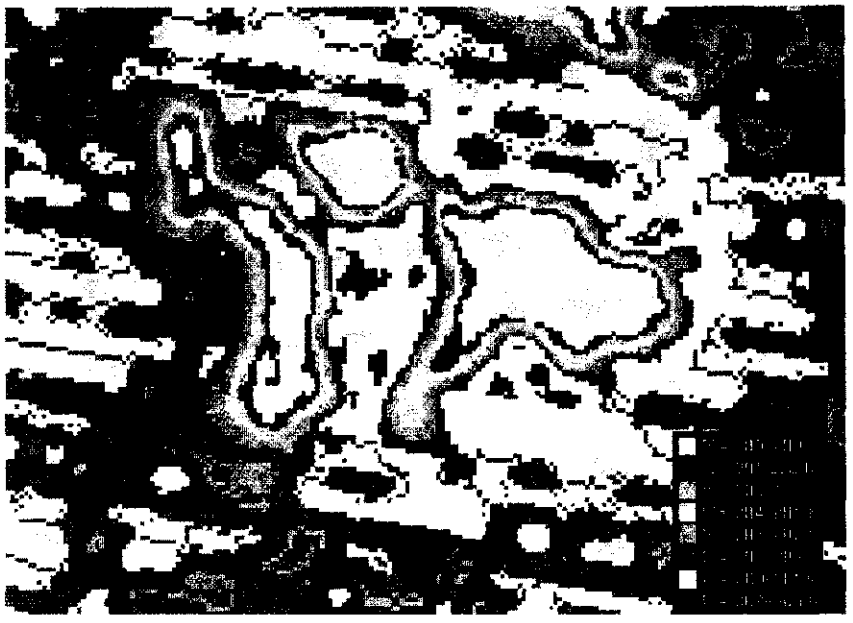

Fig. 4. Map of surface temperature, T_0, based on data of Thematic Mapper band 6, Qattara depression, Western Desert of Egypt (13-11-1987, frame 179/39-40).

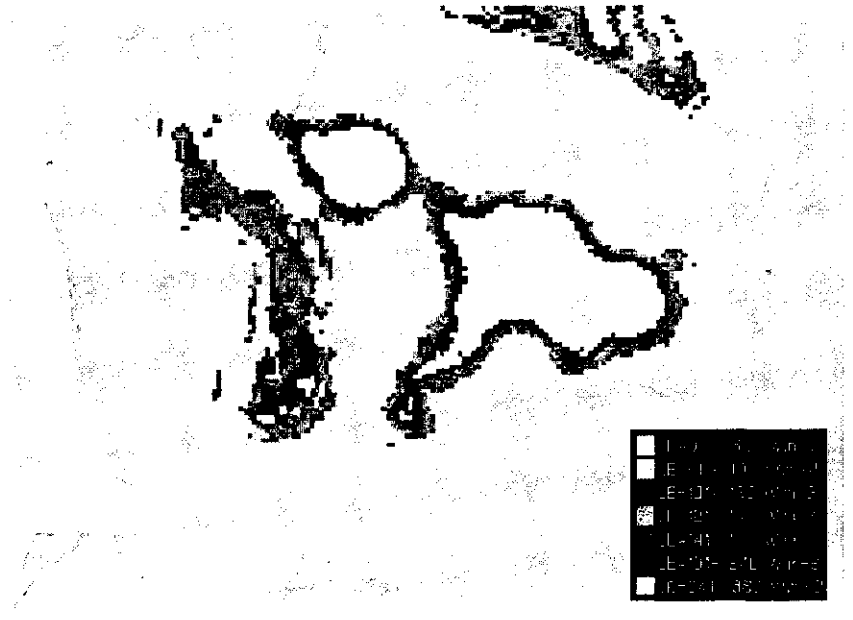

Fig. 5. Map of latent heat flux, LE, calculated with LANDSAT Thematic Mapper measurements of surface reflectance and surface temperature in the Qattara depression, Western Desert of Egypt (13-11-1987, frame 179/39-40)
L = λ = latent heat of vaporization ($J.kg^{-1}$).

Table 1, it is obvious that the pixels in the sebkha areas have a much higher evaporation than the surrounding pixels. The areal distribution of evaporation in a bounded area can be applied to analyse regional natural groundwater losses from that particular area.

5.2 Daily values

In order to obtain daily evaporation values with the instantaneous latent heat flux values, as mentioned in Section 5.1, additional data on the daily course of evaporation are necessary. Although field data on the diurnal cycle of actual evaporation of specific sebkhas are available, it is too simplistic to assume similar daily variation for non-homogeneous surface types. Therefore, a solution is sought by applying a numerical simulation model (EVADES). The EVADES-model has been developed and applied to determine the actual evaporation from soil with a dry top layer (Bastiaanssen et al., 1989). This model simulates the depth of the evaporation front and water flow in the unsaturated zone. Determination of unsaturated hydraulic conductivity and soil water retention characteristics is the main problem in describing water flow. Effective transport coefficients between the evaporation front and the soil surface are calculated. The relation between groundwater table and daily evaporation rate is obtained in the form of a look-up table (Bastiaanssen et al., 1990). Linking different predicted specific daily evaporation values (E(i), $mm.d^{-1}$) from this look-up table with predicting instantaneous latent heat fluxes ($\lambda E(i)$, $W.m^{-2}$) with the same specifications (groundwater table, soil type) on the image shown in Figure 7, generates a data set which can be fitted with the following third order polynomial function:

$$E(i) = -0.02 + 0.01\ \lambda E(i) - 3.32 * 10^{-5}\ \lambda E(i)^2 + 1.45 * 10^{-7}\ \lambda E(i)^3 \quad (6)$$

$(mm.d^{-1})$

Applying this algorithm to each pixel of the latent heat flux image, results in a map for daily evaporation (Figure 7).

The daily evaporation is significantly higher than estimations given in earlier studies (JVQ, 1981; Sundborg and Nilsson, 1985). Our evaporation values are based upon extensive field campaigns performed to study in-depth the surface energy balance and analyses of soil physical properties in sebkha areas.

5.3 Yearly values

Information of the yearly evaporation is more relevant in the framework of groundwater losses, than daily values are. To estimate the yearly evaporation, the procedure outlined in Section 5.2 must be repeated for different periods of the year. This requires a set of available satellite images. An alternative simple procedure, is to make use of the known yearly cycles of meteorological variables e.g. solar radiation and air temperature. This is not straightforward since evaporation depends on the radiation budget ($\lambda E = f(Q^*)$). One has to accept that this approach is less accurate.

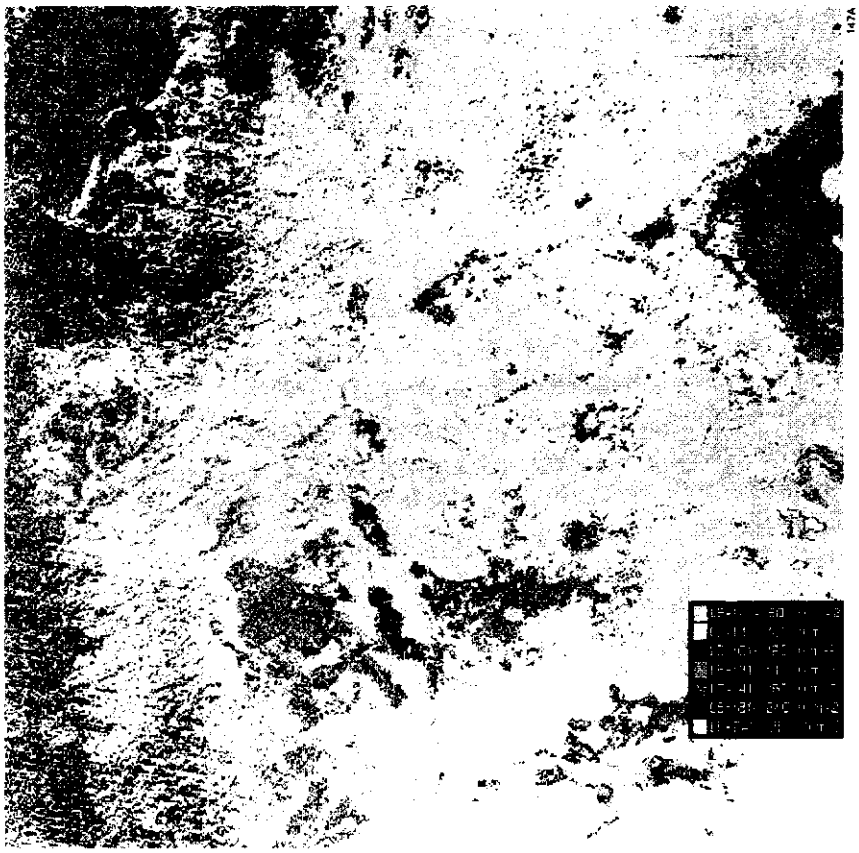

Fig. 6. Map of latent heat, LE, for the total area between Qara oasis and Bir Qifar, Qattara depression, Western Desert of Egypt, obtained after LANDSAT Thematic Mapper measurements (13-11-1987, frame 179/39-40)
$L = \lambda$ = latent heat of vaporization ($J.kg^{-1}$).

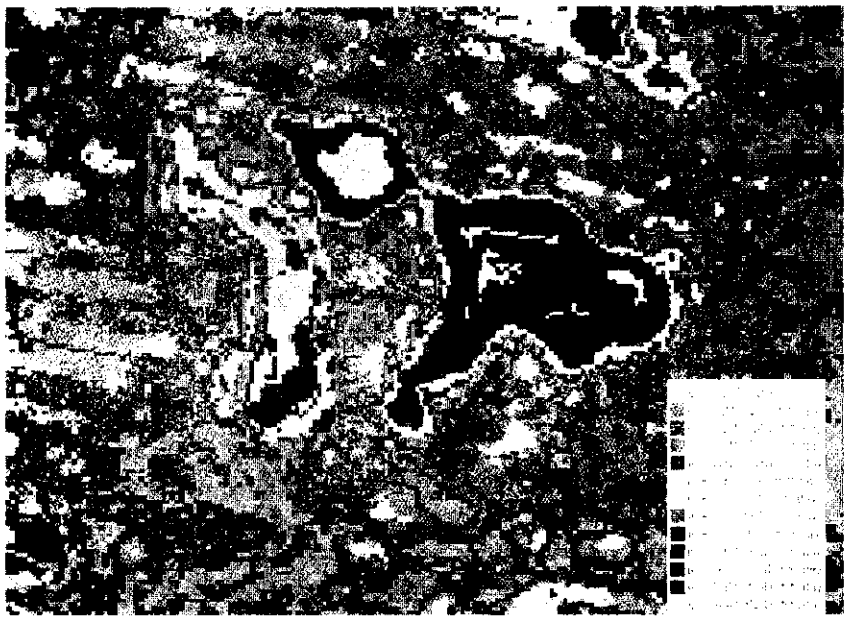

Fig. 7. Detailed map of daily evaporation, e ($mm.d^{-1}$) for an area in the Qattara depression, Western Desert of Egypt (13-11-1987). This map is based on LANDSAT Thematic Mapper observations and result of hydrological simulation models.

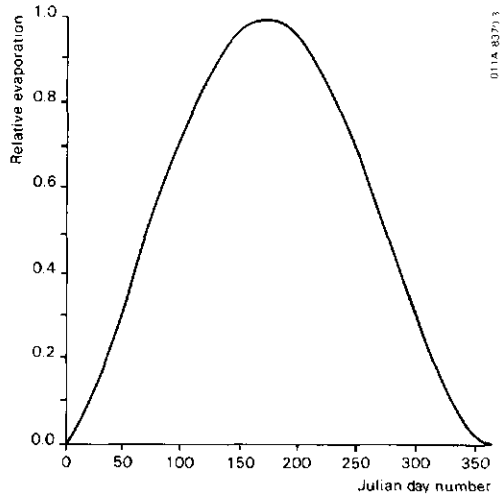

Fig. 8 The yearly distribution of evaporation based on the cycles of solar radiation for Siwa and Qara oases, Western Desert of Egypt.

An example based on the yearly variation of solar radiation has been worked out for the oasis of Qara. The yearly trend of evaporation is assumed to be equal to the yearly trend of solar radiation as known from the meteorological station at Siwa (Figure 8).

The yearly evaporation of the Qara oasis was estimated on the relation drawn in Figure 8 and minimum (e_{rel} = 0.0) and maximum (e_{rel} = 1.0) values of evaporation for different levels of groundwater as given in Table 3. The relationship between evaporation and groundwater table depth was obtained by simulation results with the EVADES-model. The yearly amplitude of evaporation (A(E)) varies with the depth of the groundwater table and soil type (Table 3). This implies that $\lambda E = f(A(E), K\downarrow)$ is also acceptable with deeper groundwater tables, since the effect of the yearly K↓-cycle is persuaded by the small amplitude of the yearly evaporation cycles. For groundwater deeper than 5 meter below surface level (A(E) = 0.0 mm.d^{-1}), effects of K↓ are not present at all.

Table 3 Estimated range of minimum and maximum values of daily evaporation for different types of sebkha and related depth of the groundwater table.

Groundwater table (cm below the soil surface)	e_{min} (e_{rel} = 0) (mm.d^{-1})	e_{max} (e_{rel} = 1) (mm.d^{-1})	Yearly amplitude (mm.d^{-1})	Yearly evaporation (cm.yr^{-1})
6	3.5-4.0	7.2-8.3	3.7-4.3	201-232
30	0.8-1.2	1.7-2.6	0.9-1.4	32- 72
50	0.5-0.9	1.1-1.8	0.5-0.9	29- 52
200	0.0-0.3	0.0-0.8	0.0-0.5	0- 17

Table 4 Annual natural groundwater losses in the Qara oasis, Western Desert of Egypt. Estimations are based on satellite images in combination with hydrological simulation models.

Yearly evaporation ($cm.yr^{-1}$)	Area (ha)	Natural discharge ($Mm^3.yr^{-1}$)	Relative coverage (%)
0- 6	252	0.14	3.6
7-14	4051	4.68	58.2
15-22	1922	3.48	27.6
23-30	486	1.27	7.0
31-38	122	0.42	1.8
39-46	53	0.23	0.8
47-54	34	0.17	0.5
55-70	34	0.21	0.5
71-86	11	0.08	0.2
Total	6965	10.68	100.2

The yearly losses from the area covering the total Qara oasis can be estimated when the spatial distribution of soil specific yearly evaporation is known. This was possible after linking up the yearly evaporation (Table 3) with the image of latent heat flux (Figure 6). The natural losses of Qara oasis are presented in Table 4.

The yearly evaporation of Qara oasis (10.7 $Mm^3.yr^{-1}$) is high in comparison with the natural losses of the southern part of the Qattara depression (90 $Mm^3.yr^{-1}$) and Siwa oasis (18.3 $Mm^3.yr^{-1}$). This agrees with the conclusions drawn in Section 5.2, that the natural losses are one order of magnitude higher than indicated in Table 1. This is probably due to the fact that no extensive fieldwork on the surface energy balance and unsaturated soil water flow was carried out during previous investigations.

Expressing the result of Table 4 into average daily values, gives 0.42 $mm.d^{-1}$ on a yearly basis. Latter value agrees rather well with the average evaporation of subarea 10 and 19 with respectively 0.0 $mm.d^{-1}$ and 0.79 $mm.d^{-1}$ of a finite element model for saturated groundwater flow in the Qattara region (Pelgrum, 1988). The natural sink of groundwater in this subareas of the network cannot be compared with the natural losses presented in Table 4 since the subareas do not exactly match the topographic boundaries of Qara oasis.

6 CONCLUSIONS: IMPACT OF NATURAL EVAPORATION LOSSES ON GROUNDWATER DEVELOPMENT IN THE WESTERN DESERT OF EGYPT

An accurate knowledge of the quantities of evaporation from sebkhas is required to develop regional groundwater development plans. Through LANDSAT Thematic Mapper imagery it was possible to classify dominant types of sebkha with surface reflectance and surface temperature. On the basis of these variables, it was also possible to define an algorithm to obtain maps of instantaneous evaporation on a pixel by pixel base. It can be concluded that although sebkhas have a dry top layer, the evaporation front is rather shallow and the actual evaporation has a large impact on the groundwater balance. It has been shown that with remote sensing techniques in addition to field observations, natural groundwater losses can be better assessed than by applying classical groundwater modeling methods with sketchy knowledge of deep non-homogeneous aquifer system characteristics. Natural losses in general have to be revised in relation to the physical character of sebkhas and related depth of the groundwater table. Artificial extraction will affect the depth of the groundwater table and occurrence of wet sebkhas.

In order to make optimum use of groundwater resources in the oases, development plans have been worked out by the Ministry of Development in the New Valley of Egypt. It appears that 105,000 feddan in addition to the present cultivated area of 42,000 feddan could be reclaimed (Euroconsult/Pacer, 1983). Plans dealing with the East Uweinat area have shown that 189,000 feddan could be cultivated with available groundwater (GPC, 1984). The area around Lake Nasser is suitable for the reclamation of 75,000 feddan (Soliman, 1987). According to the General Petroleum Company, the Goverment plans to increase the total extraction in the Western Desert from 417 $Mm^3.yr^{-1}$ in 1980 to 2359 $Mm^3.yr^{-1}$ in the nearby future (GPC, 1986). All this data are based upon groundwater flow with low natural losses as presented in Table 1 and calculated by simulating groundwater flow over a period of time shorter than the time required to reduce groundwater losses in the sebkhas (because of the extraction-induced drawdown).

It is very clear that groundwater flow is affected by natural evaporation, which has to be considered in the future groundwater development plans. Since this study with analyses of physical transport processes in dry soils, supported with the regional interpretation by means of satellite images, has shown that sebkhas have an important impact on the total groundwater availability, reclamation schemes have to be revised.

ACKNOWLEDGEMENTS

The research of this publication was financed by the Dutch Ministry for Development Cooperation, who also shares copyright. Citation is encouraged. Short excerpts may be translated and/or reproducted without prior permission, on the condition that the source is indicated. For translation and/or reproduction in whole the Section for Research and Technology of the aforementioned Ministry (P.O. Box 20061, 2500 EB The Hague, the Netherlands) should be notified in advance.

Responsibility for the contents and for the opinions expressed rest solely with the authors and their organizations; publication does not constitute and endorsement by the Dutch Ministry for Development Cooperation.

The essential financial support of the Dutch Remote Sensing Board (BCRS) is gratefully acknowledged. The LANDSAT Thematic Mapper data have been provided by NASA in the framework of the NASA program 'Thematic Mapper Research in the Earth Sciences'.

The authors would like to acknowledge Dr. Massimo Menenti for his constructive comments on specific details of this paper.

REFERENCES

Abd El Karim, M.H. 1989. Mapping evaporation from playas in the Western Desert: approach and practical examples. Note 1972. The Winand Staring Centre for Integrated Land, Soil and Water Research, Wageningen, the Netherlands. 41 pp.

Ball, J. 1931. The Qattara depression of the Lybian Desert and the possibility of its utilization for power production. Geogr. J. LXXII.4.

Bastiaanssen, W.G.M., P. Kabat and M. Menenti. 1989. A new simulation model of bare soil evaporation in deserts, EVADES. Note 1938. The Winand Staring Centre for Integrated Land, Soil and Water Research, Wageningen, the Netherlands. 73 pp.

Bastiaanssen, W.G.M. and M. Menenti. 1989. Surface reflectance and surface temperature in relation with soil type and regional energy fluxes. In: A.F. Bouwman (ed.). Soils and the greenhouse effect. John Wiley & Sons, Chichester, UK: 541-549.

Bastiaanssen, W.G.M., M. Menenti and P. Kabat. 1990. Simulation of capillary soil water flow under arid conditions: application to soil types in the Western Desert of Egypt. Proc. Symp. on Land drainage for salinity control in arid and semi-arid regions, Cairo, Egypt.

Brinkmann, P.J., M. Heinl, R. Hollander and G. Reich. 1987. Groundwater model for the Nubian Aquifer system. IWAWI, Sonderforschungsbereich 69, Berlin, West Germany. 58 pp.

EUROCONSULT/PACER. 1983. Regional development plan for New Valley. Final report. Ministry of Development. Cairo, Egypt.

GPC (General Petroleum Company of Egypt). 1984. Assessment of groundwater resources of the Nubian aquifer - East Uweinat area, South West Egypt. Report to Government.

GPC (General Petroleum Company of Egypt). 1986. Foreseen extraction plans, Western Desert of Egypt. Unpublished map. Cairo, Egypt.

Heinl, M. and J. Brinkmann. 1989. A groundwater model of the Nubian aquifer system. Hydrol. Sc. J. 34,4: 425-447.

JVQ (Joint Venture Qattara. 1981. Study Qattara Depression; Feasibility Report. Lahmeyer International Consultant. Volumes 1-4.

List, F.K., D. Linne and B. Meissner. 1989. LANDSAT-TM study of sabkha surfaces in the Qattara depression, Northwestern Egypt. Proc. Workshop 'Earthnet pilot project on Landsat Thematic Mapper applications', December 1987, Frascati, Italy: 99-110.

Menenti, M. 1984. Physical aspects and determination of evaporation in deserts applying remote sensing techniques. Ph.D. Thesis and Report no. 10 (Special Issue). Institute for Land and Water Management Research, Wageningen, the Netherlands. 202 pp.

Menenti, M. and W.G.M. Bastiaanssen. 1989. Estimation of effective properties of non-homogeneous land surfaces with measurements of surface reflectance and temperature. 40th Congress of the International Astronautical Federation, 7-12 October, Malaga, Spain. 9 pp.

Menenti, M., W.G.M. Bastiaanssen, D. van Eick and M.H. Abd El Karim. 1989. Linear relationships between surface reflectance and temperature and their application to map actual evaporation of groundwater. Adv. Space Res. 9.1: 165-176.

Menenti, M., A. Lorkeers and M. Vissers. 1986. An application of Thematic Mapper data in Tunesia, estimation of daily amplitude in near-surface soil temperature and discrimination on hypersaline soils. ITC-Journal 1986-1: 35-42.

Michels, B.I. 1989. CHESS or how to calculate atmospheric correction from global radiation data in desert areas. Internal Report 19. The Winand Staring Centre for Integrated Land, Soil and Water Research, Wageningen, the Netherlands. 51 pp.

Pelgrum, G.H. 1988. Groundwater flow in the Qattara depression area, Western Desert of Egypt. Wageningen Agricultural University, Wageningen, the Netherlands. 38 pp.

Price, J.C. 1982. On the use of satellite data to infer surface fluxes at meteorological scales. J. Appl. Meteor. 21(8): 1111-1122.

RIGW-WSC. 1989. Hydrogeological synthesis of the Western Desert of Egypt. Joint report Research Institute for Groundwater, Cairo and The Winand Staring Centre for Integrated Land, Soil and Water Research, Wageningen, the Netherlands. 94 pp.

Roeters, P.B. 1987. Determining soil moisture conditions of salt crusts by using Landsat TM data, a qualitative and quantitative approach. Note 1753. Institute for Land and Water Management Research, Wageningen, the Netherlands. 41 pp.

Soliman, M.M. 1987. Groundwater model of area adjacent to Aswan High Dam reservoir. Report to Research Institute for Groundwater, Cairo, Egypt.

Sundborg, A. and B. Nilsson. 1985. Qattara Hydrosolar Power Project Environmental Assessment. UNGI Report 62. Uppsala University, Uppsala, Sweden. 194 pp.

Timmerman, K.B. 1989. Standardization of the albedo. Internal Publication 26. The Winand Staring Centre for Integrated Land, Soil and Water Research, Wageningen, The Netherlands. 25 pp.

Zeeman, M. 1989. Berekening en classificatie van oppervlakte reflectie-beelden met behulp van Landsat TM-data: case study Quattara-Depressie (Egypte). Internal Publication 20. The Winand Staring Centre for Integrated Land, Soil and Water Research, Wageningen, The Netherlands. 31 pp.